

Incommensurability and atomic structure of $c(2 \times 2)\text{N}/\text{Cu}(100)$: A scanning tunneling microscopy study

T. Choi, C. D. Ruggiero, and J. A. Gupta

Department of Physics, The Ohio State University, Columbus, Ohio 43210, USA

(Received 21 May 2008; revised manuscript received 17 June 2008; published 17 July 2008)

We use a scanning tunneling microscope operating in a low-temperature ultrahigh vacuum environment to study the atomic structure of single layer films of Cu_2N grown on $\text{Cu}(100)$. The $c(2 \times 2)$ lattice of Cu_2N is incommensurate, with a lattice constant of 0.372 ± 0.001 nm that is 3% larger than the bare $\text{Cu}(100)$ surface. This finding suggests that the strain due to lattice mismatch contributes to self-assembly in this system. We find that the image contrast on Cu_2N islands depends on bias voltage, which reconciles several interpretations in the literature. We assign features in these STM images to the Cu, N, and hollow sites in the Cu_2N lattice with the aid of coadsorbed CO molecules. This atomic registry allows us to characterize four different defects on Cu_2N , which influence the sticking coefficient and electronic coupling of adsorbates.

DOI: [10.1103/PhysRevB.78.035430](https://doi.org/10.1103/PhysRevB.78.035430)

PACS number(s): 68.37.Ef, 68.43.Hn, 68.55.aj, 61.46.-w

I. INTRODUCTION

Ultrathin insulating films enable nanoscale control over the coupling of adsorbates to the surface electron density of metal substrates.¹⁻³ For example, adsorbates on insulating films experience reduced hybridization, allowing direct imaging of molecular orbitals similar to the free molecule¹ and spin-flip spectroscopy of single atoms.² Tunneling spectroscopy indicates that despite being only one monolayer thick, films of adsorbed nitrogen on Cu act as an insulator with a band gap exceeding 4 eV (Ref. 4). This property has been exploited to decouple the magnetic moment of atomic-scale structures from surface electron density.³

Adsorbed nitrogen on $\text{Cu}(100)$ self assembles on two distinct length scales. At low coverage, nitrogen atoms self-assemble into small irregular islands, which exhibit a $c(2 \times 2)$ lattice. We refer to these islands as “copper nitride” or Cu_2N . With increasing coverage and annealing, the islands become nearly square shaped with an average area of $\sim 25 \pm 5$ nm² (Refs. 5 and 6). The islands themselves self assemble into a gridlike array, which has attracted interest for nanoscale templating.⁷ At saturation coverage, the islands coalesce into quasicontinuous monolayer films, which exhibit trench defects. Despite considerable interest in this system, the mechanisms for self-assembly are not well understood. Electrostatic interactions due to charge transfer,^{8,9} work-function differences,¹⁰ strain due to an incommensurate lattice,⁵ intrinsic differences in surface stress tensors,¹¹ and other surface relaxations¹² have been considered as factors contributing to the self-assembly in this system.

While scanning tunneling microscopy (STM) is useful for identifying assembly mechanisms, the interpretation of STM images of Cu_2N has also been debated. Based on coadsorption studies, Leible *et al.*⁵ have proposed that the STM images N atoms as protrusions. In contrast, Driver and Woodruff¹³ have proposed a rumpling model based on STM images showing two distinct sets of protrusions with (1×1) periodicity assigned to Cu atoms. A difficulty with both of these room-temperature STM studies is the uncertain termination of the tip. More recently, in low-temperature STM measurements by Hirjibehedin *et al.*,³ protrusions were as-

signed to hollow sites between Cu and N atoms, which are based on a lattice required to consistently account for island boundaries.

Here we present STM measurements of the $\text{Cu}_2\text{N}/\text{Cu}(100)$ system, which address the longstanding uncertainties in atomic structure and imaging contrast. After careful calibration, our STM images indicate that the lattice of Cu_2N is not commensurate with $\text{Cu}(100)$. This suggests that strain due to lattice mismatch contributes to the self assembly of islands in this system. Our STM images show a reversal in contrast with voltage, which reconciles the disparate interpretations in Refs. 3, 5, and 13. Using coadsorbed carbon monoxide (CO) molecules, we can assign features in our images to the Cu and N lattices. This atomic registry is used to characterize four different types of defects that are commonly seen in the Cu_2N islands.

II. EXPERIMENT

All measurements were made with a Createc UHV LT-STM, which operates at a temperature of 5.5 K in an ultrahigh vacuum environment ($< 1 \times 10^{-10}$ mbar). Under these conditions, thermal drift and sample contamination are negligible. The bias voltage V refers to the sample voltage. A cut Ir tip was prepared with field emission and controlled contact with the sample. The $\text{Cu}(100)$ surface was prepared by repeated Ar^+ sputtering and annealing cycles (~ 600 °C). Auger-electron spectroscopy was used to monitor sample cleanliness and N absorption. Cu_2N islands were grown by sputtering the clean Cu sample in a N_2 atmosphere (1×10^{-5} mbar) for two minutes. The high voltage of the sputter gun dissociates N_2 , so that N atoms are deposited onto the Cu surface. After nitrogen adsorption, the sample is annealed to 350 °C for one minute. Cu_2N islands were isolated on the surface at an average coverage of 0.16 ML. The sample is then cooled to 80 K and inserted into the cold STM. Carbon monoxide molecules are coadsorbed onto the surface in the STM at 12 K through a leak valve. CO molecules are identified by before/after images of the same area and inelastic electron-tunneling spectroscopy of the characteristic frustrated rotation and translation modes.¹⁴

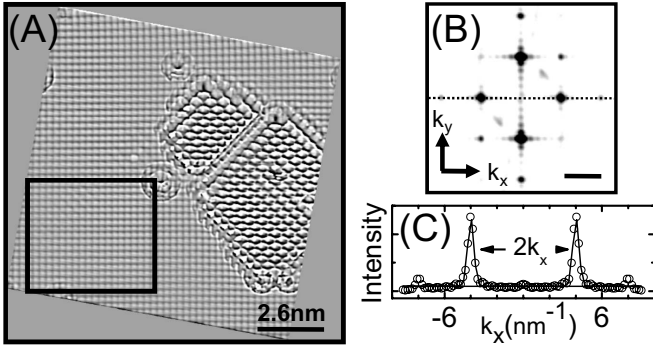


FIG. 1. (a) STM image (+25 mV, 2.4 nA) with simultaneous atomic resolution on bare Cu(100) and Cu₂N islands using a CO-terminated tip. The image was low pass and Laplace filtered to emphasize local contrast and rotated by 10.3° to align the Cu lattice. (b) 2D FFT of the selected region in Fig. 1(a). Scale bar=3.7 1/nm. (c) Horizontal linecut of the FFT spot profile and Gaussian fit (solid line). The measured values of $2/2k_x = a_{Cu_x} = 0.250$ nm and $2/2k_y = a_{Cu_y} = 0.246$ nm are used for calibrating the STM images in Figs. 2 and 3.

Atomic resolution imaging of Cu(100) was used to calibrate our STM images. To resolve metal atoms in close-packed surfaces such as Cu(100), the STM tip must be brought nearly into point contact ($R \sim 100$ k Ω). Thus, under typical imaging conditions ($R > 10$ M Ω), the lattice of Cu atoms is not directly observed. Instead we deliberately transfer a coadsorbed CO molecule from the surface to the tip by applying a voltage pulse. Such a functionalized tip exhibits enhanced contrast as a result of chemical interactions between the molecule and the surface.¹⁵ With a CO-terminated tip, we are readily able to image the (1 \times 1) lattice of Cu(100) [e.g., Fig. 1(a)]. Images are rotated by 10.3° to correct for the scan angle before further analysis.

We analyzed four ~ 50 nm² regions of Cu(100) that were free from point defects and were at least two atomic rows away from Cu₂N islands. The x and y directions were measured independently to account for differences in the sensitivity of the piezoelectric scan tube. Within our resolution, the two scan directions were orthogonal and the piezoresponse was independent of the dc offset voltage (± 150 V), which is applied to select the scan area. We measure $2k_x$ and $2k_y$ from Gaussian fits to the spot profile in the two-dimensional fast Fourier transform (2D FFT) [Figs. 1(b) and 1(c)]; an uncertainty of $\Delta k = 0.01$ nm⁻¹ is estimated based on pixelation of the fast Fourier transform (FFT) (Ref. 16). The standard deviation from the mean is 0.2% for the apparent lattice constants $a_{Cu_{x,y}} = 1/k_{x,y}$. Images were scaled by the ratio of the accepted lattice constant for clean Cu ($a_{Cu} = 0.255$ nm) to the mean apparent lattice constants $a_{Cu_{x,y}}$. Care was taken to ensure constant temperature after calibration because the scan tube's sensitivity exhibits hysteresis of a few percent after temperature cycling.

III. RESULTS AND DISCUSSION

A. Incommensurate lattice

Figure 2(a) shows an STM image of a Cu₂N island. A series of bright protrusions corresponding to the $c(2 \times 2)$ lat-

tice of Cu₂N can be resolved by a metal tip under typical imaging conditions (e.g., $R > 100$ M Ω). We measured the lattice constant of 26 Cu₂N islands ranging in area from 6–25 nm² by 2D FFT. We find no systematic variation of lattice constant with island size in this range. The mean lattice constant is $a_{Cu_2N} = 0.371$ nm, with a standard deviation of 0.005 nm and a standard deviation from the mean of 0.001 nm. This is a simple conservative estimate of random errors in our data. We have also performed a weighted average where we calculate the uncertainty in each measurement from the least-squares error in the Gaussian fit to the FFT spot profile. In principle, this accounts for the size-dependent variation in Δk (~ 0.05 – 0.1 nm⁻¹) due to the finite number of lattice points. This procedure gives $a_{Cu_2N} = 0.372 \pm 0.001$ nm, which is not appreciably different than the simple estimate which treats all data points as equivalent. Our measurement of a_{Cu_2N} is smaller than the closest bulk counterpart Cu₃N (0.381 nm), but is larger than expected for a commensurate (2 \times 2) lattice on Cu(100) (0.361 nm).

For a commensurate (2 \times 2) lattice, the ratio $a_{Cu_2N}/a_{Cu} = \sqrt{2} = 1.41$; our measured value of 1.46 ± 0.01 indicates that the Cu₂N lattice is incommensurate, independent of systematic errors in the calibration procedure. For example, a contraction of the bare Cu regions by 0.5%–1.2%, suggested by the photoemission experiments of Sekiba *et al.*,¹⁷ would proportionately decrease a_{Cu_2N} , but would not change the ratio. Therefore, surface strain due to lattice mismatch should contribute to self-assembly in this system, a suggestion first made by Leibsle *et al.*⁵ This has been a point of contention in the literature, due in part to significant uncertainty about the exact atomic structure of Cu₂N, which could not be quantified in the early STM measurements. A low-energy electron diffraction (LEED) study suggested a perfectly commensurate structure,¹⁸ although subsequent Rutherford channeling studies by the same group suggested a significant (~ 0.01 nm) vertical and lateral expansion of the Cu lattice in Cu₂N (Refs. 11 and 19). Density functional theory (DFT) (Refs. 8 and 9) and x-ray measurements suggest that nitrogen atoms sit above the plane of Cu atoms, although measured heights vary from 0–0.06 nm (Ref. 5). The uncertainty in nitrogen height translates to an uncertainty in the Cu₂N lattice constant. X-ray measurements report a bond length of $d_{Cu-N} = 0.185$ nm (Ref. 20), which corresponds to 0.35 nm $< a_{Cu_2N} < 0.37$ nm, depending on the nitrogen height one chooses. We do not directly measure d_{Cu-N} in our STM measurements, but our value of $a_{Cu_2N}/2 = 0.186$ nm sets a lower limit for this value, which is attained assuming coplanar N and Cu atoms.

B. Contrast reversal and atomic site assignment

Figures 2(a)–2(c) show STM images of the same Cu₂N island at different sample voltage. Inspection of these images reveals that the series of protrusions, which exhibit the $c(2 \times 2)$ periodicity, depend on the voltage. This is clearly seen in the insets, which show exactly the same area of the island at each voltage. Depressions at positive voltage become protrusions at negative voltage and vice versa. At low voltage

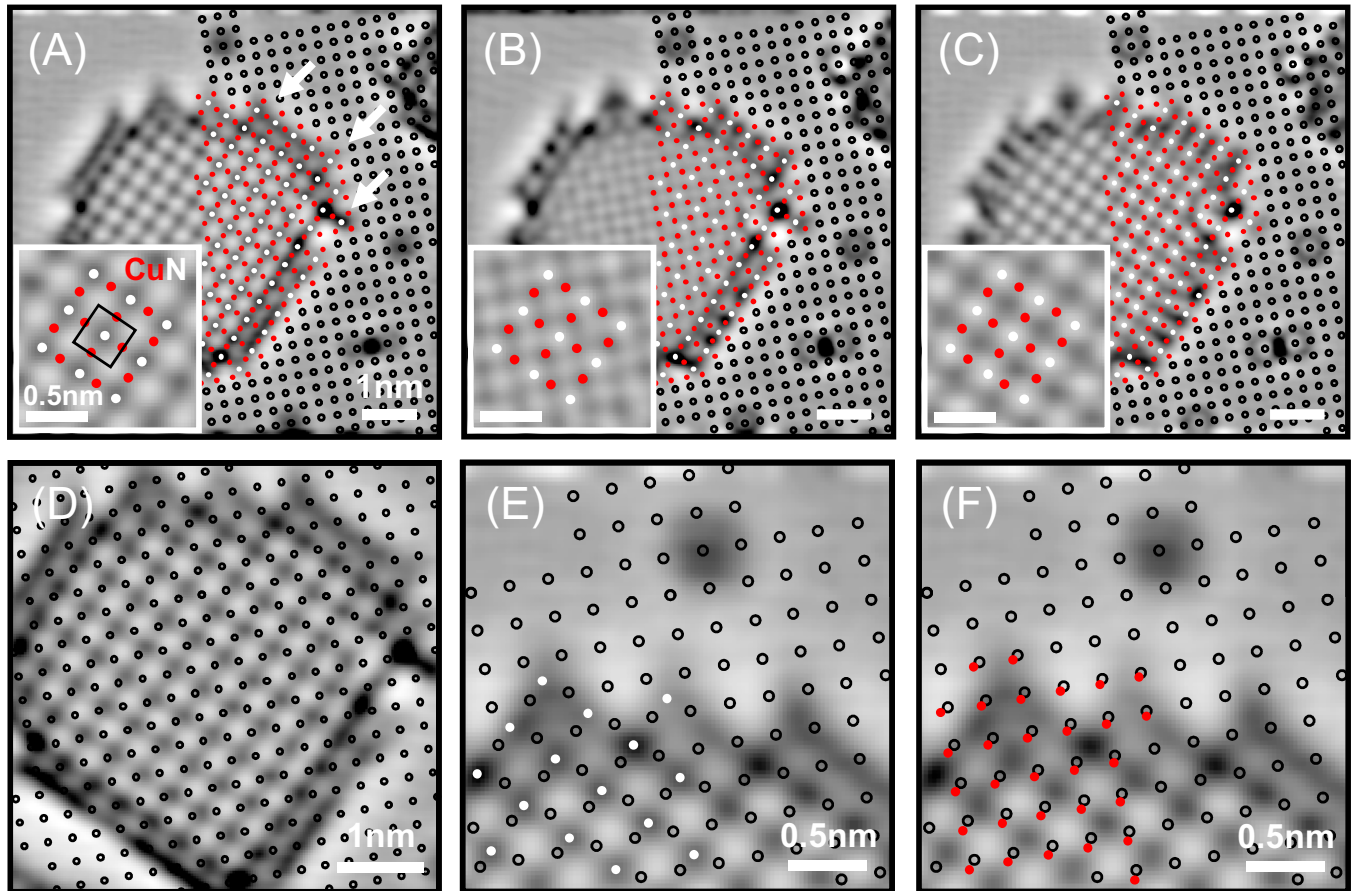


FIG. 2. (Color online) STM images of a Cu_2N island on $\text{Cu}(100)$. Open circles indicate the lattice of copper atoms on $\text{Cu}(100)$, inferred from the positions of five marker CO molecules [e.g., depression at top center of part (a)]. Red, solid dots show copper atoms within the Cu_2N island and white dots represent nitrogen atoms, according to the lattice assignment described in the text. Arrows indicate boundary features used to assign the nitrogen lattice. Insets show a higher magnification image of the island center and the unit cell. (a) +0.5 V, 2 nA. (b) -0.1 V, 1.5 nA. (c) -0.5 V, 6 nA. (d), (e), and (f) Higher magnification images of Fig. 2(a). (d) Shows the variable registry of the $\text{Cu}(100)$ lattice, and (e) the assignment of N and (f) Cu lattices in Cu_2N .

[Fig. 2(b)], we observe two sets of protrusions, defining a (1×1) lattice.

Exact registry of Cu atoms in the bare surface with the features in Cu_2N islands is needed to interpret these images. STM images with simultaneous atomic resolution on Cu and Cu_2N surfaces provide the simplest way to obtain this registry [e.g., Fig. 1(a)]. However, in our experience, simultaneous atomic resolution is only possible with an adsorbate-terminated tip. While useful for calibration, we believe such tips are not reliable for assigning adsorption sites because the chemical contrast mechanism can vary with the surface and tip adsorbate.

We instead coadsorb a well-studied reference adsorbate to determine binding sites in the Cu_2N islands (Ref. 5). CO molecules are known to adsorb atop Cu atoms on $\text{Cu}(100)$ (Ref. 14). Five CO molecules are situated near the Cu_2N island in Fig. 2. The $\text{Cu}(100)$ lattice (open circles) is inferred from the position of these CO molecules, with a spacing and rotation as determined in our calibration measurements of bare $\text{Cu}(100)$ regions.

Incommensurability complicates the registry of features in the STM images of Cu_2N with the $\text{Cu}(100)$ substrate. Close inspection of Fig. 2(d) reveals that if we extend the inferred

$\text{Cu}(100)$ lattice across the Cu_2N island, the registry of Cu lattice points varies, as expected for incommensurate lattices. We assign the depressions at positive voltage [Figs. 2(a) and 2(d)–2(f)] to nitrogen atoms based on two criteria:

(1) Proximity to hollow sites: Experiment and theory agree that nitrogen atoms adsorb at the fourfold symmetric hollow sites on $\text{Cu}(100)$ (Refs. 5, 8, and 9). Figure 2(e) indicates that both depressions and protrusions in the (2×2) lattice lie nearest the hollow sites. *A priori*, either one of these could be assigned to nitrogen atoms.

(2) Consistency with island boundaries: We distinguish between these choices by considering the island boundary.³ At positive voltage, atomically sharp depressions form corners along the islands' perimeter [arrows in Fig. 2(a)]. In STM images where we inhibit island formation by reduced annealing temperature, we find that individual nitrogen atoms are imaged as depressions at positive voltage. Thus, we locate the lattice of nitrogen atoms (solid, white dots) as needed to consistently account for the sharp corners in Fig. 2(a).

The lattice of Cu atoms within the Cu_2N island (solid, dark red dots) is chosen in a similar fashion. In this case, if we extend the bare Cu lattice onto the Cu_2N island, imaged

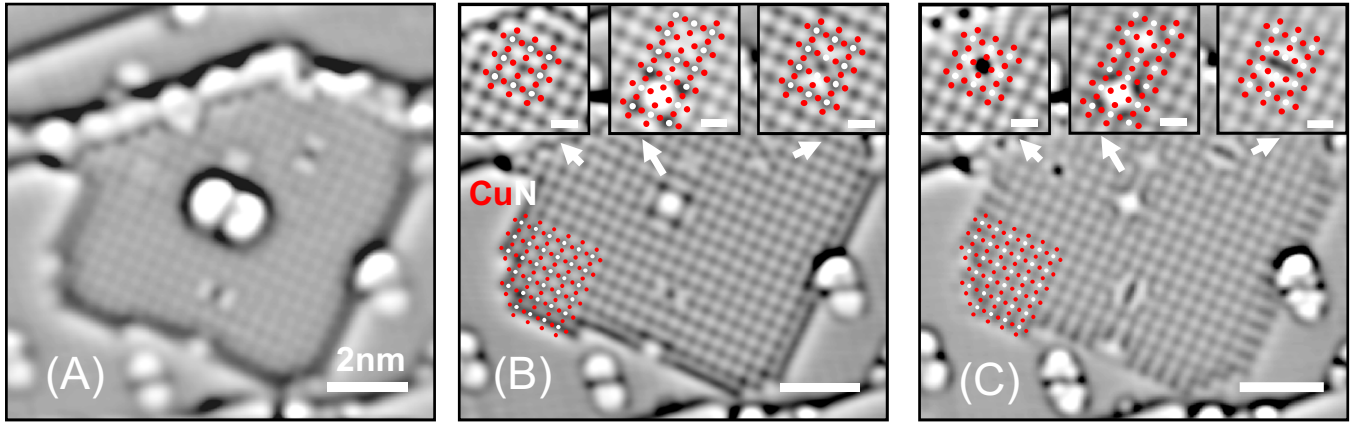


FIG. 3. (Color online) STM images of defects in a Cu_2N island. (a) An azobenzene molecule adsorbed on a Cu_2N island with several defects. $V=+0.5$ V and $I=0.1$ nA. (b) and (c) The molecule is transferred to the tip with a voltage pulse, revealing an underlying defect. The molecule-terminated tip increases resolution, but does not change the electronic contrast. Insets show four typical defects (scale bar = 0.5 nm), together with the assigned Cu_2N lattice. (b) +0.5 V, 0.1 nA. (c) -0.5 V, 0.1 nA.

at positive or negative voltage, Cu sites lie nearest the bridge positions in the (2×2) lattice [Fig. 2(f)]. This is consistent with the required (1×1) periodicity for features assigned to the Cu atoms.

We thus define the Cu_2N lattice shown in Fig. 2. Protrusions at positive voltage [Fig. 2(a)] locate hollow sites between Cu and N atoms, while protrusions at negative voltage [Fig. 2(c)] locate N atoms. This lattice assignment, together with our observation of voltage-dependent contrast, reconciles the interpretations in Refs. 3, 5, and 13. The assignment of protrusions at negative voltage to nitrogen atoms agrees well with DFT calculations,^{8,21} although the contrast reversal we observe was not reproduced in the calculations. Prior STM (Ref. 6) and DFT studies²¹ suggest a nonuniform expansion of the Cu_2N (2×2) lattice. However, the uniform lattice shown in Fig. 2 fits well to the entire island. We suggest that any lattice distortion is limited to regions near the boundaries, which do exhibit distinct contrast in STM images.

Figure 2(b) shows a more complicated (1×1) periodicity at low voltage. To eliminate possible artifacts, which vary with tip height, we adjusted the set current so that the tip height over Cu_2N was identical in Figs. 2(b) and 2(c). From our lattice assignment, we see that both nitrogen and hollow sites are imaged simultaneously as protrusions at low voltage. Such images were first observed by Driver and Woodruff,¹³ who developed a rumpling reconstruction model in which both sets of protrusions were assigned to Cu atoms. Our measurements instead indicate that this is an electronic contrast effect.

We note a correspondence of these images with voltage-dependent contrast in GaAs(110) (Ref. 22). There, it was observed that the STM images occupied valence states (i.e., As atoms) at negative voltage and unoccupied conduction states (Ga atoms) at positive voltage. In our STM measurements of insulating Cu_2N (Ref. 4), valence states are associated with nitrogen atoms and conduction states are associated with the empty hollow sites, perhaps reflecting leakage of state density from the underlying Cu substrate.

C. Defects in Cu_2N films

Defects play an important role in the properties of few-monolayer insulating films. Not only can defects define conducting channels through the insulating film, they can also affect the interaction between surface and adsorbates. For example, oxygen vacancies on MgO films promote charge transfer to adsorbed metal clusters, which influences their catalytic activity.²³ Adsorbates may also preferentially stick to these defects due to the higher electron density available for bonding.

To characterize these effects, we adsorbed an organic molecule, azobenzene ($\text{C}_{12}\text{H}_{10}\text{N}_2$), on the $\text{Cu}_2\text{N}/\text{Cu}(100)$ surface. Consistent with studies in other systems,²⁴ we find that azobenzene preferentially sticks to exposed Cu regions, with a ratio of $\sim 25:1$. The few molecules we find on Cu_2N islands are typically tethered to defects in the Cu_2N film. For example, Fig. 3(a) shows an STM image of an azobenzene molecule on a Cu_2N island. This molecule was transferred to the STM tip by applying a voltage pulse. Subsequent imaging with the molecule-terminated tip indicates that the azobenzene molecule was adsorbed atop a defect in the Cu_2N film [Figs. 3(b) and 3(c)]. The spatial resolution in these images is improved by the molecule-terminated tip, although the electronic contrast remains identical to the bare tip images (Fig. 2).

While on average, we observe <0.3 defects per island, the island in Fig. 3 happened to have all four of the defects we commonly observe. Using our lattice assignment, we propose origins for two of the defects. For clarity, we refer to the appearance of these defects at negative voltage [Fig. 3(c)]. We attribute a twofold symmetric depression centered on Cu sites to a Cu vacancy (right inset). We observe three different fourfold symmetric defects centered at the nitrogen site. We attribute a ~ 0.02 nm protrusion (center inset, top) to a N vacancy based on our observation that such defects can be created by applying a voltage pulse >3 V to the STM tip. We are not able to resolve a nitrogen atom on the surface after this procedure, but it is possible that the atom desorbs completely or falls back to the surface away from our scan

area. The two other less common defects at the nitrogen lattice site appear as a ~ 0.03 nm depression (left inset) and a higher ~ 0.06 nm protrusion (center inset, bottom). These may be substitutional defects or associated with subsurface Cu impurities underneath the Cu_2N island.

IV. CONCLUSIONS

These STM measurements address some of the debate concerning the self-assembly and interpretation of STM im-

ages in the $\text{Cu}_2\text{N}/\text{Cu}(100)$ system. The $c(2 \times 2)$ lattice is shown to be incommensurate, with a lattice constant of 0.372 ± 0.001 nm. The variation in image contrast with voltage reconciles the disparate interpretations in prior STM studies and allows us to assign a lattice of Cu and N atoms within the islands.

ACKNOWLEDGMENTS

We are grateful to the NSF for support through CAREER Grant No. DMR-0645451.

-
- ¹J. Repp, G. Meyer, S. M. Stojković, A. Gourdon, and C. Joachim, *Phys. Rev. Lett.* **94**, 026803 (2005).
²A. J. Heinrich, J. A. Gupta, C. P. Lutz, and D. M. Eigler, *Science* **306**, 466 (2004).
³C. F. Hirjibehedin, C. P. Lutz, and A. J. Heinrich, *Science* **312**, 1021 (2006).
⁴C. D. Ruggiero, T. Choi, and J. A. Gupta, *Appl. Phys. Lett.* **91**, 253106 (2007).
⁵F. M. Leibsle, S. S. Dhesi, S. D. Barrett, and A. W. Robinson, *Surf. Sci.* **317**, 309 (1994).
⁶F. Komori, S. Ohno, and K. Nakatsuji, *Prog. Surf. Sci.* **77**, 1 (2004).
⁷T. M. Parker, L. K. Wilson, N. G. Condon, and F. M. Leibsle, *Phys. Rev. B* **56**, 6458 (1997).
⁸Y. Yoshimoto and S. Tsuneyuki, *Surf. Sci.* **514**, 200 (2002).
⁹A. Soon, L. Wong, B. Delley, and C. Stampfl, *Phys. Rev. B* **77**, 125423 (2008).
¹⁰D. Vanderbilt, *Surf. Sci.* **268**, L300 (1992).
¹¹B. Croset, Y. Girard, G. Prevot, M. Sotto, Y. Garreau, R. Pinchaux, and M. Sauvage-Simkin, *Phys. Rev. Lett.* **88**, 056103 (2002).
¹²H. Ellmer, V. Reparin, S. Rousset, B. Croset, M. Sotto, and P. Zeppenfeld, *Surf. Sci.* **476**, 95 (2001).
¹³S. M. Driver and D. P. Woodruff, *Surf. Sci.* **492**, 11 (2001).
¹⁴L. J. Lauhon and W. Ho, *Phys. Rev. B* **60**, R8525 (1999).
¹⁵H. J. Lee and W. Ho, *Science* **286**, 1719 (1999).
¹⁶I. Horcas, R. Fernandez, J. M. Gomez-Rodriguez, J. Colchero, J. Gomez-Herrero, and A. M. Baro, *Rev. Sci. Instrum.* **78**, 013705 (2007).
¹⁷D. Sekiba, Y. Yoshimoto, K. Nakatsuji, Y. Takagi, T. Iimori, S. Doi, and F. Komori, *Phys. Rev. B* **75**, 115404 (2007).
¹⁸M. Sotto and B. Croset, *Surf. Sci.* **461**, 78 (2000).
¹⁹C. Cohen, H. Ellmer, J. M. Guigner, A. L'Hoir, G. Prevot, D. Schmaus, and M. Sotto, *Surf. Sci.* **490**, 336 (2001).
²⁰T. Lederer, D. Arvanitis, M. Tischer, G. Comelli, L. Tröger, and K. Baberschke, *Phys. Rev. B* **48**, 11277 (1993).
²¹Y. Yoshimoto and S. Tsuneyuki, *Appl. Surf. Sci.* **237**, 274 (2004).
²²R. M. Feenstra, J. A. Stroscio, J. Tersoff, and A. P. Fein, *Phys. Rev. Lett.* **58**, 1192 (1987).
²³B. Yoon, H. Hakkinen, U. Landman, A. S. Worz, J. M. Antonietti, S. Abbet, K. Judai, and U. Heiz, *Science* **307**, 403 (2005).
²⁴N. Nilius, T. M. Wallis, and W. Ho, *Phys. Rev. Lett.* **90**, 046808 (2003).